

NASA Technical Memorandum 107213
AIAA-96-1740

A Unique Ducted Fan Test Bed for Active Noise Control and Aeroacoustics Research

Laurence J. Heidelberg
*Lewis Research Center
Cleveland, Ohio*

David G. Hall, James E. Bridges, and M. Nallasamy
*NYMA, Inc.
Brook Park, Ohio*

Prepared for the
Second Aeroacoustics Conference
cosponsored by the American Institute of Aeronautics and Astronautics and the
Confederation of European Aerospace Societies
State College, Pennsylvania, May 6-8, 1996



National Aeronautics and
Space Administration

A Unique Ducted Fan Test Bed for Active Noise Control and Aeroacoustics Research

Laurence J. Heidelberg *
National Aeronautics and Space Administration
Lewis Research Center
Cleveland, OH 44135

David G Hall,** James E. Bridges,**
and M. Nallasamy*
NYMA, Inc.
Brook Park, OH 44142

Abstract

This paper describes a unique, large diameter, low speed, axial fan test bed with an externally supported duct. This fan can be used both to investigate active noise control and for more general fan aeroacoustics research. Several of the features and the design philosophies are presented. The most important feature is the installation of two mode measuring systems that enable the complete modal structure (all circumferential and radial orders) of both the inlet and exhaust ducts to be determined.

A sample of data for two configurations, rotor alone and rod/rotor interaction are presented. In-duct modal data for rotor alone reveals minimal extraneous modes that might interfere with any interaction modes being investigated. The rod data shows strong interactions for the expected modes. High resolution spectral and spacial far-field data reveal a directivity pattern consistent with the modal structure. The unique ability to view both far-field and in-duct modal structure makes this test bed well suited for the test and development of fan active noise control systems.

The rod modal data was projected to the far-field using a finite element code and compared to the actual far-field data showing an excellent agreement. This not only validates the code but contributes to confidence in the in-duct and far-field data quality.

Introduction

Development of the next generation of commercial transport aircraft will require an extensive effort in the area of engine noise reduction. As part of NASA's Advanced Subsonic Technology Noise Reduction Program, technology is being developed to reduce engine noise 6 EPNdB relative to certified levels as of 1992. The trend towards ultra-high-bypass engines with short and thin nacelles is making it difficult to provide adequate passive acoustic treatment for noise reduction. At the same time, noise regulations are becoming more stringent. One possible solution to this dilemma is Active Noise Control (ANC) of the fan tones. This will require the verification of in-duct active noise control techniques, and the use of advanced technology in Computational Aeroacoustics (CAA). To support this effort, a ducted fan test bed with a number of unique features has been developed at NASA's Lewis Research Center. This test bed, referred to as the ANCF (Active Noise Control Fan), consists of a large, low-speed ducted fan driven by an electric motor, rotating rake mode measurement systems and an inlet flow control device to allow static testing. It is housed in the APL (Aeroacoustic Propulsion Laboratory) facility at NASA Lewis; a hemi-anechoic chamber with provisions for far-field noise measurements.

Research in both the areas of ANC and CAA can benefit from less complicated duct acoustics, geometry, and high Mach number flows. The low fan tip speed, simple duct lines, and low axial velocity were chosen to simplify the problems but not lose the

* Senior Member, AIAA. ** Member, AIAA.

essential acoustics of an aero propulsion fan. Thus, the modal structure of the ANCF duct acoustics has both circumferential (spinning) as well as radial modes but a lower number than would be present in a high-speed fan. The ANCF is an intermediate step to full scale engine testing of fan active noise control.

Apparatus and Procedures

The ANCF has several unique features that set it apart from all other fan noise test beds; the rotating rake mode measurement system (with inlet/exhaust capability), the size and operating frequency range, the capability to run with a wide variety of stators or rods in the duct (including no stators), variable pitch rotor blades, and the use of an Inflow Control Device to permit static testing. Photographs of ANCF are shown in Figure 1 with both the ICD installed and a bare inlet.

Structure and Drive Train

The ability to test the rotor alone with no vanes or struts in the duct made for a difficult structural and acoustic problem. The load path between the fan and the duct had to be long. The fan had to be rigidly supported to maintain tight blade tip clearances (0.03 in). These problems were solved with the structure and drive train shown in a top view in Figure 2. The relatively light weight fan centerbody and a heavy tube that supports the duct are connected by a horizontal strut. This strut is almost two fan diameters downstream of the rotor to minimize its interaction with the blade wakes. The strut is also acoustically shielded by the fan centerbody, since the far-field microphones are on the opposite side of the support structure. In addition, any residual wake/strut interaction noise is radiated vertically and therefore minimized in the direction of the microphones.

The drive consists of a 125 horsepower electric motor, and two drive shafts connected by a belt. The motor is located as far away as possible from the rotor to lower the mass at the end of the fan centerbody. The motor is driven by a variable frequency AC controller with the ability to set speed to

± 0.2 RPM.

A column supports the fan and associated structure at a centerline height of 10 ft. The column rests on a moveable base that provides the ability to move the ANCF from the far-field arena when only in-duct testing is required.

Fan Rotor and Duct

The fan duct and rotor of the ANCF is shown in Figure 3. The rotor is a commercially available ventilating fan with 16 composite blades. This 4 foot diameter fan has a maximum tip Mach number of 0.35, which corresponds to a corrected speed of 1886 RPM. The blade pitch angle is adjustable over a wide range, 25-50 degrees as measured at the hub. ANCF generally uses blade angles between 40 and 50 degrees with a corresponding inlet duct Mach number range of 0.10 to 0.13. The fan hub/tip ratio is 0.307, and the average blade chord is 4.5 inches.

The duct has a constant diameter over the entire length for simplicity. The inlet duct length can be varied from 0.3 to 1.3 L/D, where L/D is the length/diameter ratio. The exhaust duct has a fixed length of 1.0 L/D. Nozzle area contraction is accomplished by an increase in the center body diameter to where the exit plane hub/tip ratio is 0.5.

Rotating Rake Mode Measurement System

The ANCF rotating rake mode measurement system is a new implementation of the technique originally conceived by T.G. Sofrin (Ref.1). This technique allows the researcher to make comprehensive measurements of the spinning acoustic mode structure either in the duct or at the duct/far-field interface plane while minimizing invasive contamination effects. One previous implementation exists (Ref. 2), which provided results in the inlet of a sub-scale model. Development of the ANCF test bed has included the first-ever example of combined inlet and exhaust duct measurements on the same device. These measurements are critical to the development of new, low-noise aircraft engines because

tone noise suppression is highly dependent on acoustic mode control. The best way to evaluate the benefits of various, competing tone-noise control schemes is to quantify the fundamental physical phenomenon which generates them. The rotating rake mode measurement technique provides this information. Determination of true overall noise control effectiveness requires spinning mode characterization at both ends of the duct. This system is capable of measuring the complete modal structure from the blade passing frequency (BPF) through 3BPF.

As shown in Figure 2(b), there are two rakes, one in the inlet and one in the exhaust duct. These rakes are attached to a small section of the wall that rotates at exactly 1/100 of the fan speed. Microphones at 6 to 7 radial locations on the rake sense the acoustic radial pressure profile. Generally only one rake is installed at a time, and rakes are removed for far-field testing.

The radio frequency microphone telemetry signals which are transmitted across the rotating boundary to receivers in the APL facility. The receiver outputs are routed to a Digital Acoustic Data System (DADS, Ref. 3) in the APL control room. This is a unix-based workstation with a high speed Analog/Digital conversion subsystem. The ANCF is also equipped with a shaft encoder system. The encoder signals are routed to DADS and used to synchronize the digitizing of the microphone signals with the fan shaft angular location. The digitized microphone signals are stored in disk files on the workstation for post test analysis. This analysis is a two step process. The basic procedure is described in Ref. 4 but summarized here for convenience. All post-processing is performed on the DADS workstation. The spectrum of a signal observed by a stationary microphone shows peaks at the fan BPF and its harmonics. All acoustic modes in the fan duct generate noise at these frequencies, regardless of mode order. With a microphone rotating at a precise fraction of the fan speed, each circumferential mode generates a peak at a unique frequency. The key to the rotating rake mode measurement technique is precise control of the fan/rake speed ratio. A small "doppler

shift" occurs, with the degree of shift proportional to circumferential mode order (m-order) and speed ratio. The spectrum of the rotating microphone therefore shows a cluster of closely spaced tones in the vicinity of BPF and its harmonics. With the ANCF speed ratio of 100:1, the spacing between tones near BPF is 0.01 shaft orders. A difference between this system and the one in Ref 4 is that the digitizer is slaved to a fan shaft encoder.

The first step in processing the ANCF data is a high resolution spectral analysis to extract these m-orders for each microphone. Time domain averaging is used to enhance the signal-to-noise ratio while maintaining an absolute phase reference. The output from this process is a set of m-orders at each microphone location. These m-orders are then combined with the rake geometry information and used as input for the second processing step. The radial mode orders are estimated using a least-squares curve fitting program with Bessel functions corresponding to annular duct modes.

Size/Operating Frequency

The development of active noise control technology for large turbofan engines using sub-scale laboratory models is very difficult. Miniaturized versions of acoustic sources for active control often bear little resemblance to devices suitable for full-scale engines. Most active control schemes require the use of microprocessor-based digital controllers to perform adaptive, real-time signal processing. This processing is extremely challenging in a sub-scale model because the acoustic frequency of the fan increases as the physical size is scaled down. This requires an accompanying increase in digital controller bandwidth/processing speed. The ANCF avoids these problems by providing a duct diameter of about one half, and operating frequency comparable to a full-scale ultra-high-bypass ratio engine.

Stator Configurations

Most sub-scale turbofan models are ill suited for basic research in rotor-stator interaction noise because the stators perform

two functions; swirl recovery and structural support for the engine nacelle. The structural consideration usually places severe limitations on the ability to re-configure the stators for noise research purposes. The ANCF does not require any in-duct stators or structural supports. It also features a modular design to allow rapid re-configuration of the stators including axial and circumferential positioning. Any number of stator vanes up to 28 (currently) may be installed in the exhaust duct at any axial location from 0.5 to more than 4.0 rotor chords downstream of the trailing edge of the rotor blades. The vanes have a chord length equal to the average rotor blade chord, 4.5 inches. In addition, the stator vane assembly can be rotated to any angular position (clocked) so as to rotate an azimuthal directivity pattern in the far-field. Rods can be installed upstream of the rotor to insure that a strong and well-understood wake-pressure pattern impinges on the rotor and generates acoustic modes. This can facilitate validation of mode-prediction CAA codes.

Inflow Control Device

Another important feature of the ANCF is the ICD (Inflow Control Device, Ref. 5). The ICD removes large scale, random turbulence and ground vortices that would otherwise interact with the rotor and cause extraneous tone noise to be generated. The shape of the ICD represents an equal potential surface as determined by a potential flow code. The ICD is composed of 11 identical segments of compound curved honeycomb panels attached to very thin ribs. This does generate a very weak but predictable fixed-pattern flow distortion at the fan and results in some extraneous acoustic mode energy. This 11 lobed fixed distortion pattern results in no propagating modes below 2BPF. One of the first milestones in the development of the ANCF was to measure this energy and account for it in future experiments featuring noise suppression techniques. Control measures intended for in-duct noise sources will not necessarily work on noise originating due to external flow distortions. Results showing the magnitude of the ICD/rotor interactions will be presented in a later section of this paper. A 22 section ICD that

should have no interaction modes below 3BPF will be tested shortly.

The ICD allows testing without the need for a simulated freestream in-flow. This results in the following major advantages over test beds that require a wind-tunnel environment to simulate forward aircraft flight:

- 1) The absence of any freestream airflow reduces the level of background noise present in far-field measurements.
- 2) Low background levels allow the ANCF to be designed with inexpensive, lightly loaded composite rotor blades and a low-power drive motor.
- 3) Rig operation is fairly quiet, even before the application of any noise suppression measures. This allows test support personnel to work around the rig while it is running.

Aeroacoustic Propulsion Laboratory (APL)

The APL facility is a 130 ft diameter geodesic dome at NASA Lewis enclosing several test stands (Ref. 6). The ANCF makes use of various facility instrumentation systems including electrical power and a computerized acoustic data acquisition system. The APL includes a fully anechoic acoustic arena with treated walls and floors and a far-field microphone array at a nominal radius of 50 ft and an angular resolution of approximately 6 deg.

Results and Discussion

Baseline acoustic data resulting from two test configurations are reported in this paper: rotor alone, and 14 rods mounted upstream of the rotor. In part, this data is presented for the purpose of demonstrating the capabilities and quality of the ANCF systems. A companion paper, Ref.7 reports the results of several stator vane configurations and the same rotor as in this investigation. The inlet and exhaust in-duct modal structure from BPF to 3BPF, as well as far-field narrowband measurements were taken from 1520 to 1886 RPM. In addition, the 14 rod modal data projected to the far-field using a finite element code is compared to the actual far-field data. All the data

shown is for the rotor set to a blade pitch angle (as measured at the hub) of 40 degrees.

Comparison of the Modal Structure of Rotor Alone Versus Rod/Rotor Interaction

The inlet modal structure at BPF measured at the entrance (upstream end of the constant area section) of the inlet is compared at the maximum corrected speed of 1886 RPM in Figure 4. The modal structure is portrayed in the form of a 3-D bar graph with the mode power, PWL referenced to 10^{-12} watts plotted against both circumferential (m) and radial (n) orders. The expected $m=2$ order due to the wakes of 14 rods interacting with 16 rotor blades at BPF dominates all other modes by almost 25 dB. The rotor alone modes can be seen to all be at or below 90 dB (level at which measurement reliability becomes low). These low levels indicate there are few and weak sources extraneous to rod/rotor interaction. Examples of extraneous sources include inlet flow distortions and variations in blade tip clearance. The back row in the plots show the total power in the m-order and the total power in the tone is shown above each plot. The rotor alone is almost 30 dB below the 14 rods in terms of total tone PWL. This very large difference is due in part to a clean aerodynamic fan installation and a strong rod/rotor interaction. The 14 rods show a higher number/level of extraneous modes than rotor alone. This might be related to a higher level of turbulence in the fan inflow. Figure 5 shows the same comparison for 2BPF. The interaction for the 14 rod case should occur at $m=4$. This m-order is composed of two radial orders and dominates over the other modes. The largest of the extraneous modes is at $m=2$ with a total level below 100dB or almost 20 dB below the rod/rotor interaction. For the rotor alone, the 11 segment ICD interaction should occur at $m=-1$ and is evident by two of the three radial orders above 90 dB. The rotor alone levels are higher than at BPF but still well below the 14 rod data. The 3BPF modal comparison is shown in Figure 6 where, as might be expected, there are many more modes present. The 14 rods should produce interactions at $m=6$ & -8 , which are quite evident in the data. The total PWL for each of these m-orders is almost identical and they

are, by far, the major contributors to the total tone power. The largest of the extraneous modes is $m=4$, which happens to be an ICD interaction mode. The rotor alone shows this mode as well as a second interaction mode, $m=-7$ at levels around 95 dB. It is interesting to note the $m=4$ level for the 14 rod data is 10 dB higher than the rotor alone indicating a possible additional, but unknown source for this mode.

Figures 7-9 show the modal structure comparison for BPF through 3BPF respectively, for the exhaust duct. These measurements were taken with the rake just upstream of the exit plane. The BPF interaction mode, $m = 2$, for 14 rods is 5 dB higher than it was for the inlet. The $m=1$ is noticeably the highest of the extraneous modes (over 100 dB). This is still well below the interaction mode level. For rotor alone at BPF there are no significant modes present. The 2BPF modes for 14 rods are similar to the inlet with $m=4$ somewhat higher and the extraneous modes slightly lower. For rotor alone, at 2BPF only a small amount of $m=-1$ from the ICD is shown. The 3BPF plots are very similar to the inlet plots (Fig. 6) except for 14 rods, an extraneous mode for $m=-10$ is unusually high.

Effect of Rake Location on Mode Measurements

All the inlet mode data presented up to this point was measured at the inlet entrance or 0.72 L/D from the fan. Measurements were also made much closer to the fan at 0.208 L/D which is about half way along the fan spinner. A comparison of these measurements for BPF and 2BPF are shown in Figures 10 and 11, respectively. The 14 rod interaction mode, $m = 2$, at BPF is slightly higher near the fan than the upstream location. This could be due to a small inlet or spinner termination reflection which would create a weak axial standing wave pattern in the duct. The other modes are low and similar for both locations. The two locations have nearly the same modal structures at 2BPF. In fact, the total power in the tone is identical for both locations. The good agreement shown here contributes to confidence in the mode measuring system and

a generally low level of in-duct reflections.

Effect of Fan Speed on the Interaction Modes

The strength of the interaction modes in terms of power is shown in Figure 12 for both inlet and exhaust at BPF and 2BPF. The 14 rods generate an $m=2$ at BPF and only one radial order can propagate, (2,0). In the inlet, this mode power increases with speed up to 1700 RPM and then has a relatively flat response with increasing speed. A similar behavior is displayed in the exhaust with levels somewhat higher than the inlet. The inlet data at 2BPF shows the $m = 4$ modes from the 14 rod interaction and the $m=-1$ from the ICD. Most of these modes increase with speed from 1520 to 1886 RPM. The (4,1) mode has a more erratic behavior and has lower levels than (4,0). It should be noted that this mode is cutoff at the lowest speed shown, for the inlet only. The ICD, $m=-1$ modes are well below the 14 rod modes. The exhaust modes show similar behavior except the (4,1) mode is less erratic.

Far-field Results

Far-field noise measurements were taken over an arc of almost 170 degrees with 28 microphones resulting in an average angular resolution of approximately 6 degrees. A narrowband analysis with a resolution bandwidth of 2.2 Hz was used to create tone directivity plots for both the 14 rod and rotor alone configurations. This very narrow bandwidth allows the accurate measurement of weak tones. In addition, broadband levels near the tones were established by averaging two bands on either side of the tone base.

Figure 13 shows a summary of the far-field results for both configurations from BPF through 3BPF at maximum speed. Included on the plots are the fan broadband floor (rotor alone) and the facility background floor. Zero degrees on the plots is on the inlet axis and the radius is 10 D. The 14 rods on the BPF plot show strong lobes in both the inlet and exhaust quadrants. These lobes are caused by the (2,0) modes. A comparison of Figures 4(a) and 7(a) shows the exhaust mode to be 5 dB stronger than the inlet, which corresponds to the larger lobe seen in the far-

field exhaust. The rotor alone is generally 25 to 35 dB below the 14 rod data at angles around lobe peaks, and its relatively flat shape indicates no dominate modes are present. This is consistent with the modal structures previous presented. The fan broadband floor is generally 10 to 18 dB below the rotor alone tone. This indicates that the very narrow spectral analysis used in the far-field makes this data even more sensitive than the in-duct modal data. The higher levels seen on the 167 deg microphone for many of the tones and broadband may be suspect since this location is on the edge of the exhaust flow. The background noise is generally 20 dB below the broadband, except where the open facility door is responsible for higher levels at the end of the exhaust quadrant. The 2BPF plot for 14 rods shows a more complicated pattern than BPF. This is primarily due to the presence of two modes in both the inlet and exhaust, (4,0) and (4,1). The rotor alone curve is noticeably higher than at BPF. This again is consistent with the modal structure (Figs 5(b) and 8(b)) where the ICD modes ($m=-1$) are present. The 3BPF plots are similar to 2BPF due to the presents of multiple interaction and extraneous modes. The background noise levels drop as the frequency increases but still rise in the vicinity of the door.

Computational Aeroacoustics

The ANCF provides a valuable source of experimental data to verify Computational Aeroacoustic computer programs for fan noise prediction. These programs will permit rapid evaluation of low-noise engine designs while reducing the need to fabricate large numbers of expensive prototypes. The following categories of CAA programs are candidates for verification using the ANCF:

- 1) Those used to predict the the generation of acoustic modes and their distribution at the source. This includes modifications to include active noise control acoustic sources and to predict their effect at the source.
- 2) Those which predict the propagation of acoustic modes in the duct, including reflection/ transmission at duct terminations.
- 3) Programs to predict mode behaviour during radiation to the far-field.

A finite element code using the in-duct mode measurements for the 14 rod configuration will be used to compute the far-field directivity. These computed results are compared to the far-field measurements.

Computation of Far-Field Radiation

Inlet Radiation

Eversman and Roy (Ref 8) solve the noise radiation problem using a finite element method. The propagation in the duct and the radiation to the far-field are included in one model. The acoustic problem is formulated in terms of the acoustic perturbation velocity potential. They solve the duct eigenvalue problem for a duct with uniform flow. The formulation is a Bessel's equation of order m . The finite element solution of this equation is the approximation to the exact solution. They employ a Galerkin type finite element formulation with isoparametric elements. The mean flow is computed using a velocity potential formulation on the same mesh that is used for acoustic propagation and radiation. The acoustic field equations are written in terms of the acoustic potential and acoustic pressure and solved using finite element techniques.

The source is modeled in terms of the incident and reflected modes, which are matched to the finite element solution on the same plane. Wave envelope elements are used in the far-field, assuming that the sound field there approximates that produced by a point source. It is assumed that only outgoing waves exist at the far-field boundary, where a Sommerfeld radiation condition for a monopole in a uniform flow is applied. The same boundary conditions are applied at the baffle boundary (Ref 8). With the wave envelope elements in the far-field the entire radiation field can be modeled with a relatively small number of finite elements. The solution to the finite element system is obtained using a frontal solution method. Further details of the finite element formulation and the solution procedure may be found in Reference 8.

Aft Radiation

The equations governing the acoustic field of the aft radiation are the same as those used for the inlet. However, the jet shear

layer from the nozzle introduces complication for the computation of the mean flow. The shear layer is modeled as though the duct is extended four duct radii beyond the exit plane (Ref 9). The velocity potential is allowed to be discontinuous across the shear layer. The acoustic pressure is continuous over the entire region. Beyond this "extended" duct, the internal and external flows are allowed to mix and the velocity potential is continuous everywhere. The extent of the "extended" duct can be varied if needed.

The finite element techniques and computer codes developed by Eversman and Roy have been applied to modern turbofans (Ref 10,11) and NASA's ANCF (Ref 12).

The present computations were done on the ANCF geometry corresponding to that of the 14 rod configuration. The far-field boundary is located at 10 D (diameters) where far-field measurements are made. A long center body and a flanged exit characterize the aft duct geometry. In this study the source (input) plane is the rotating rake measurement plane of the inlet or exhaust duct. The computation is carried out separately for the inlet and aft radiation as indicated above. The propagation through the inlet and aft ducts and the respective far-field radiation are studied. A composite prediction of the far-field directivity is computed from 0 to 180 degrees, by combining the inlet and aft results. In the intermediate region where the radiation from the inlet and aft interfere with each other, the mean square pressures from the inlet and aft have been added to get the resultant curve (Ref 12). The computed far-field directivities are compared with the measurements.

Comparisons of Computed and Measured Far-field Directivities

A comparison of the computed to measured directivity for the BPF tone, for the 14 rods, at two speeds is shown in Figure 14. For both speeds, the inlet quadrant shows excellent agreement between the data and code. Both the shape and level of these curves are nearly identical. It should be pointed out that the code used only the value of the interaction mode (2,0) for this

calculation. This is adequate only when extraneous modes are very low compared to the interaction modes. All modes except the plane wave, (0,0) peak off axis. Thus, when there are tone levels above the broadband on axis, as in the 1886 RPM case, this indicates a small amount of a (0,0) mode. The agreement in the aft quadrant is not quite as good as the inlet with a tendency for the code to predict slightly more radiation at higher angles. At angles between 60 and 100 degrees both inlet and aft radiation mix and since they are coherent the possibility for interference exists. This is most evident at 1700 RPM where there are abrupt changes in directivity. If the absolute phase of both the inlet and exhaust modes had been available from the data, the code might have been able to predict this interference pattern. It should be pointed out that the relative phase between radial orders is available and was used in the code in the 2BPF case (Fig. 15).

The 2BPF comparison shown in Figure 15 represents a more complicated situation since there are two interaction modes present in the inlet and exhaust, (4,0) & (4,1). The inlet at 1886 RPM shows excellent agreement between the code and data despite a two lobe pattern. The exhaust comparison reveals a small shift to the right for the prediction as in the BPF case. As in previous plots, at 1700 RPM there is good agreement with a progressive shift to the right for the prediction as the far-field angle increases. The two lobed pattern in the inlet is missing at this speed, due to low level of the (4,1) mode.

Concluding Remarks

This paper describes a unique large diameter, low-speed, axial ducted fan test bed known as ANCF. This fan is used for both active noise control experiments and more general fan aeroacoustics research. Several of the features and the design philosophies are presented. The most important feature is the installation of two mode measuring systems that enable the complete modal structure (all circumferential and radial orders) of both the inlet and exhaust ducts to be determined for frequencies up to and including 3BPF.

A sample of data for two configurations, rotor alone and rod/rotor interaction are presented. The in-duct modal data for rotor alone reveals at BPF there are almost no modes within the sensitivity of the instrumentation. While at 2BPF and 3BPF, there are low levels of modes related to the Inflow Control Device (ICD), which is used for turbulence control. There are occasionally other extraneous modes of low level with unknown sources at the higher harmonics of BPF. The rod data shows strong interaction modes for the expected mode orders. These interaction modes were up to 35 dB higher than the other modes. The modal structure was measured at two different axial locations in the inlet duct. At both the inlet entrance, and at location near the fan, the measured modal structures were almost identical.

High resolution spectral and spatial far-field data were also obtained. These data reveal a directivity pattern consistent with the modal structure. The far-field noise floors for both the fan tone and broadband noise were more than adequate. The unique ability to view both far-field and complete in-duct modal structure makes this test bed well suited for proof of concept testing and development of fan active noise control systems.

In addition the rod interaction modal data was projected to the far-field using a finite element code was compared to the far-field data. The excellent agreement between the far-field data and the code prediction not only helps validate the code, but contributes to confidence of the in-duct and far-field data quality.

Acknowledgements

The authors would like to thank Tony Shook, Kevin Konno, and the rest of ANCF design team of NASA Lewis Research Center for their outstanding contribution to the success of this test bed.

References

- 1) Cicon, D.E., Sofrin, T.G., and Mathews, D.C., "Investigation of Continuously

Traversing Microphone System for Mode Measurement", NASA CR-168040, Nov 1982.

2) Heidelberg, L.J. and Hall, D.G., "Acoustic Mode Measurements in the Inlet of a Model Turbofan Using a Continuously Rotating Rake". *Journal of Aircraft*, Vol. 32, No. 4, 1995, pp. 761-767.

3) Hall, D. and Bridges, J. "A Sophisticated, Multi-Channel Data Acquisition and Processing System for High Frequency Noise Research". NASA CR-189137. March 1992.

4) Hall, D., Heidelberg, L., Konno, K. "Acoustic Mode Measurements in the Inlet of a Model Turbofan Using a Continuously Rotating Rake: Data Collection/Analysis Techniques". AIAA-93-0599 (NASA TM-105936). January, 1993.

5) Homyak, L., McArdle, J. and Heidelberg, L., "A Compact Inflow Control Device for Simulating Flight Fan Noise". NASA TM-83349. April 1983.

6) B.A. Cooper, "A Large Hemi-Anechoic Enclosure for Community-Compatible Aeroacoustic Testing of Aircraft Propulsion Systems". *The Journal of the Institute of Noise Control Engineering of the USA*. Jan/Feb 1994

7) Sutliff, D.L., Nallasamy, M., Heidelberg, L.J., Elliott, D.M., "Baseline Acoustic Levels of the NASA Active Noise Control Fan Rig," AIAA Paper 96-1745, May 1996; also NASA TM-107214, May 1996..

8) Eversman, W, & Roy, I.D., "Ducted Fan Acoustic Radiation Including the Effects of Non-Uniform Mean Flow and Acoustic Treatment", AIAA 93-4424, 1993.

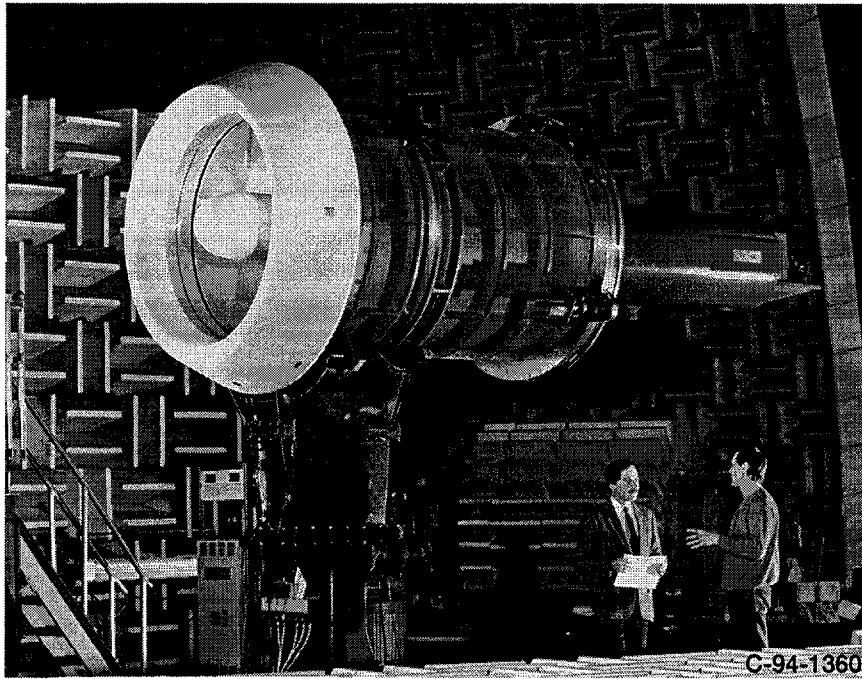
9) Eversman, W, "Aft Fan Duct Acoustic Radiation", CEAS/AIAA 95-155, 1995.

10) Philbrick D.A. & Topol, D.A., "Development of a Fan Noise Design System, Part 1: System Design and Source Modeling", AIAA 93-4415, 1993.

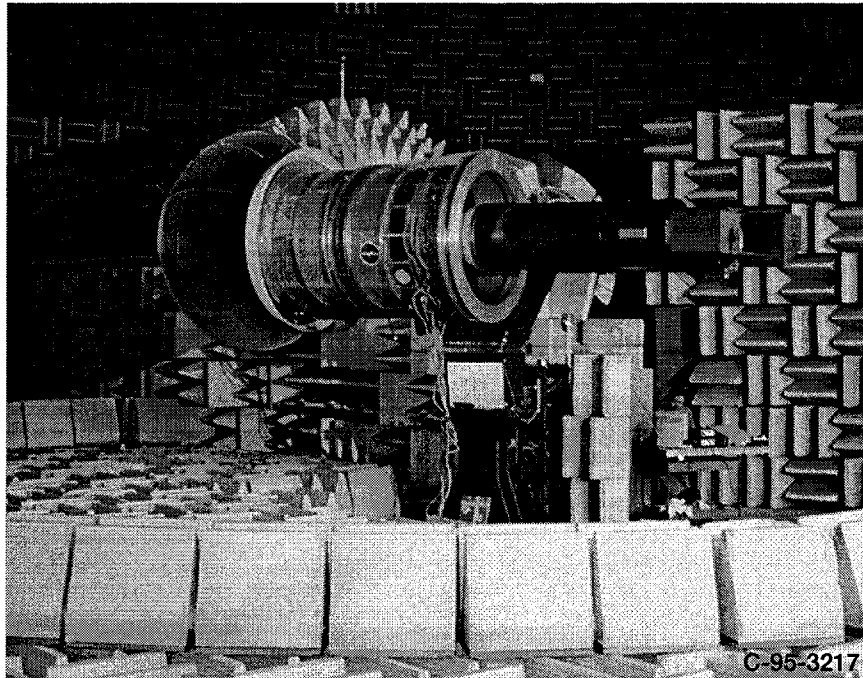
11) Topol, D.A., "Development of a Fan

Noise Design System, Part 2: Far-Field Radiation and System Evaluation," AIAA 93-4416, 1993.

12) Nallasamy, M., "Noise Radiation from Fan Inlet and Aft Ducts", AIAA Paper 96-1769, May 1996.



(a) ANCF with a bare inlet



(b) ANCF in the far-field test position with the Inflow Control Device (ICD) installed

Figure 1. Active Noise Control Fan (ANCF) Test Rig.

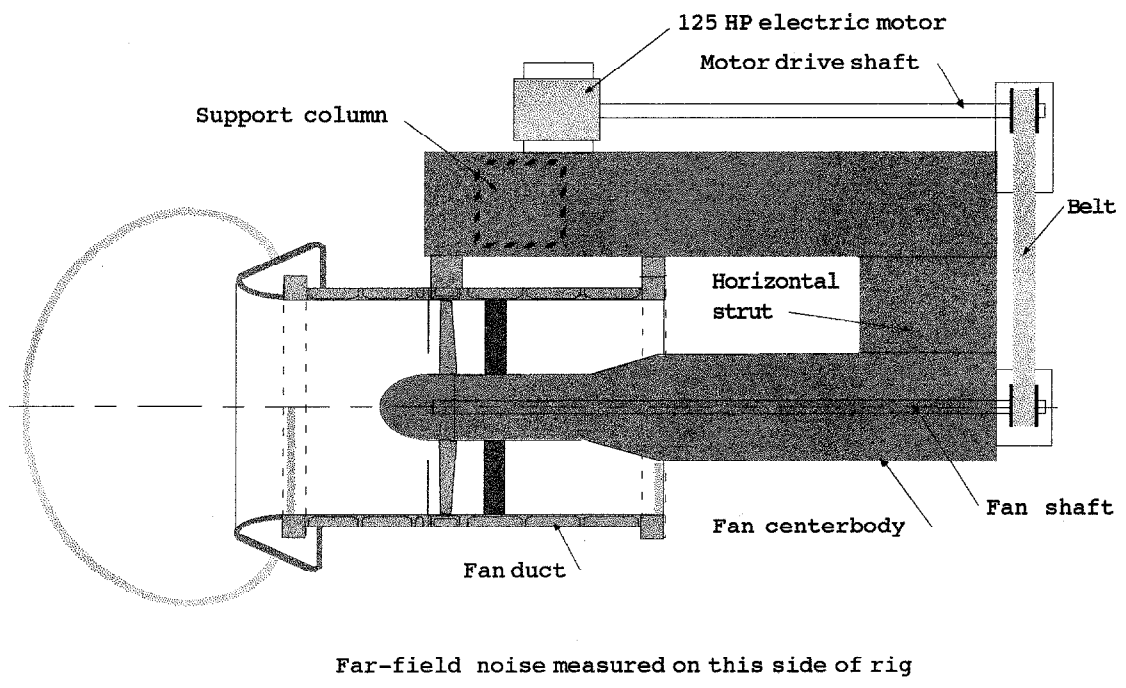


Figure 2. Top View Schematic of Active Noise Control Fan Rig Showing the Drive Train and Support Structure

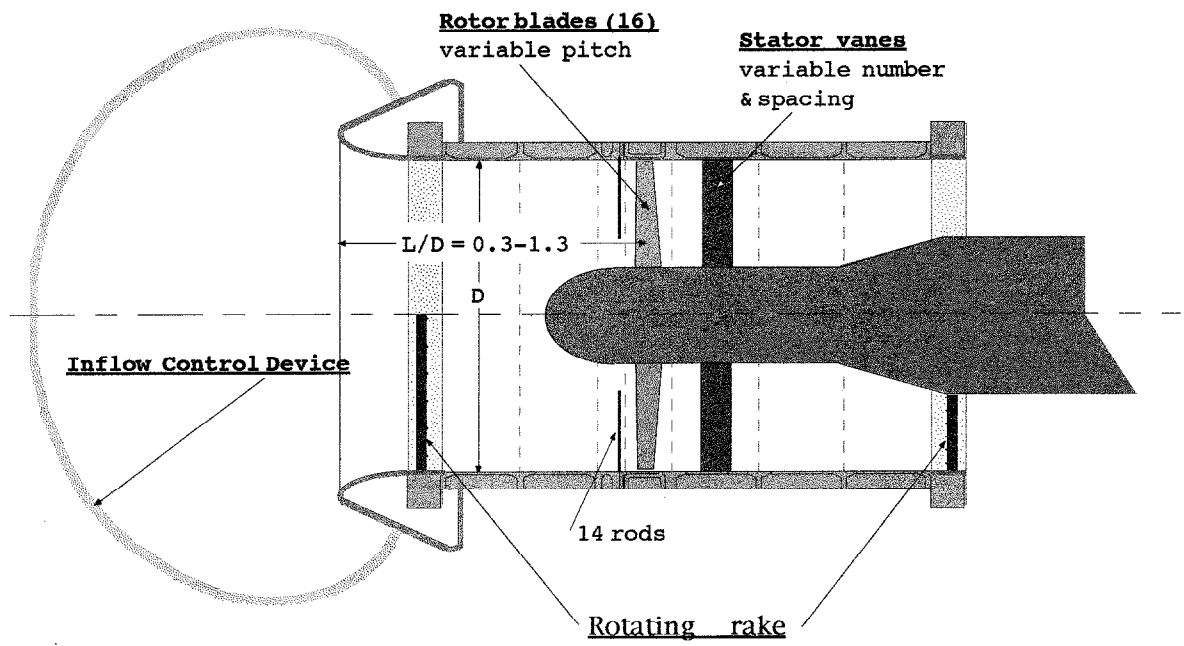


Figure 3. Schematic of Active Noise Control Fan showing Rotating Rake measurement locations

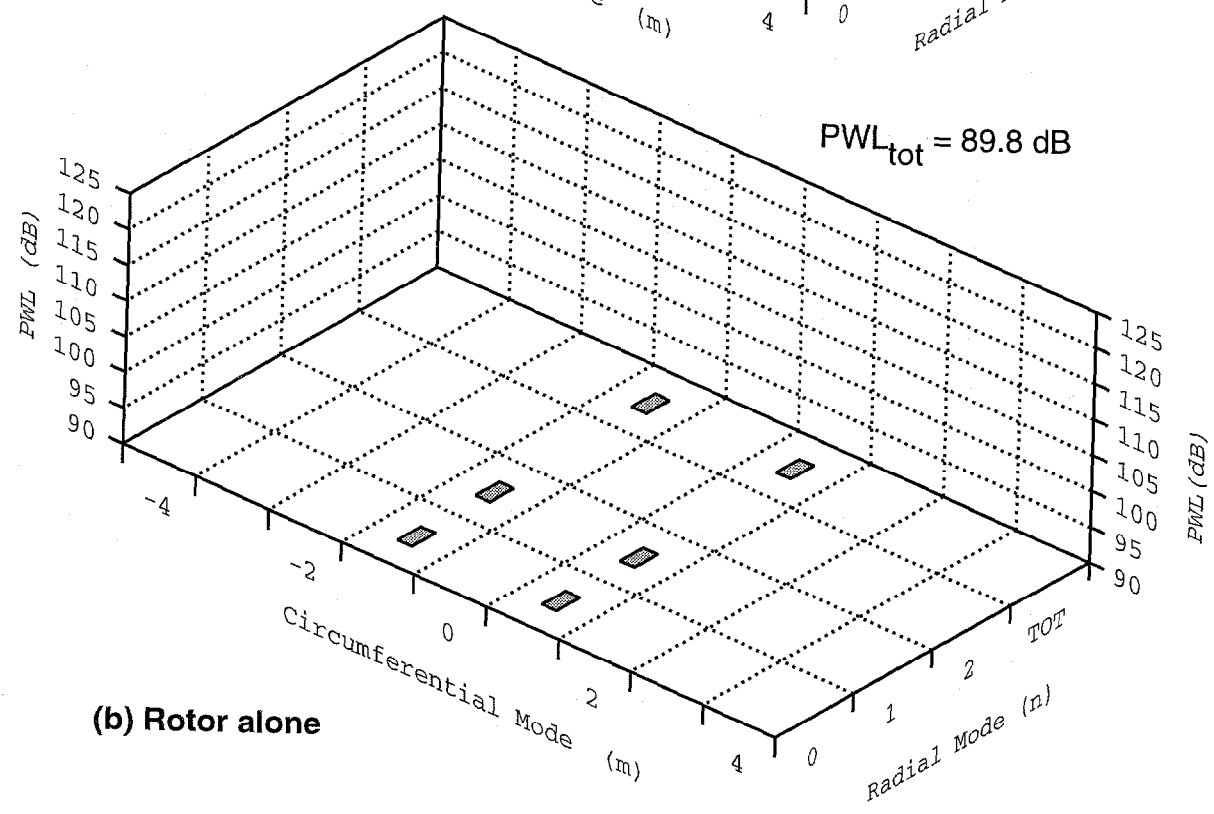
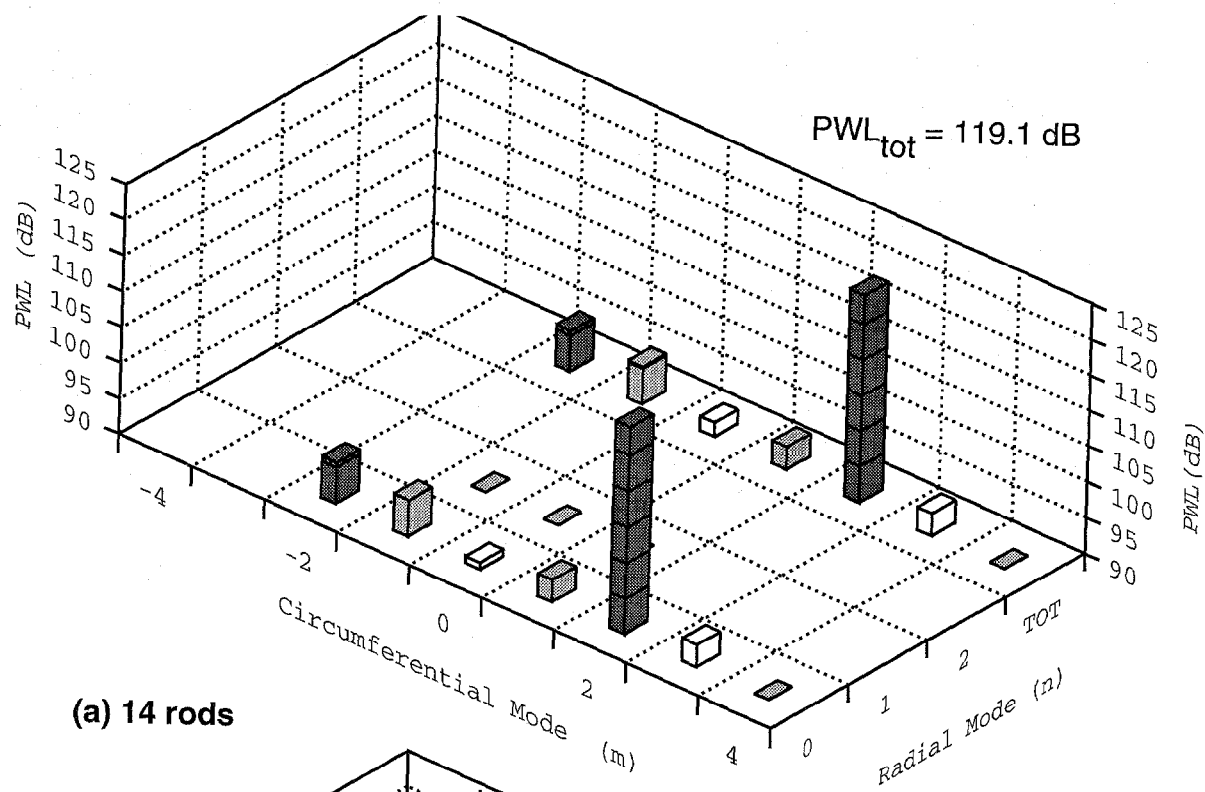


Figure 4. Comparison of Inlet Modal Structure at BPF for Rotor Alone and 14 Rod-Rotor Configurations, 1886 RPM.

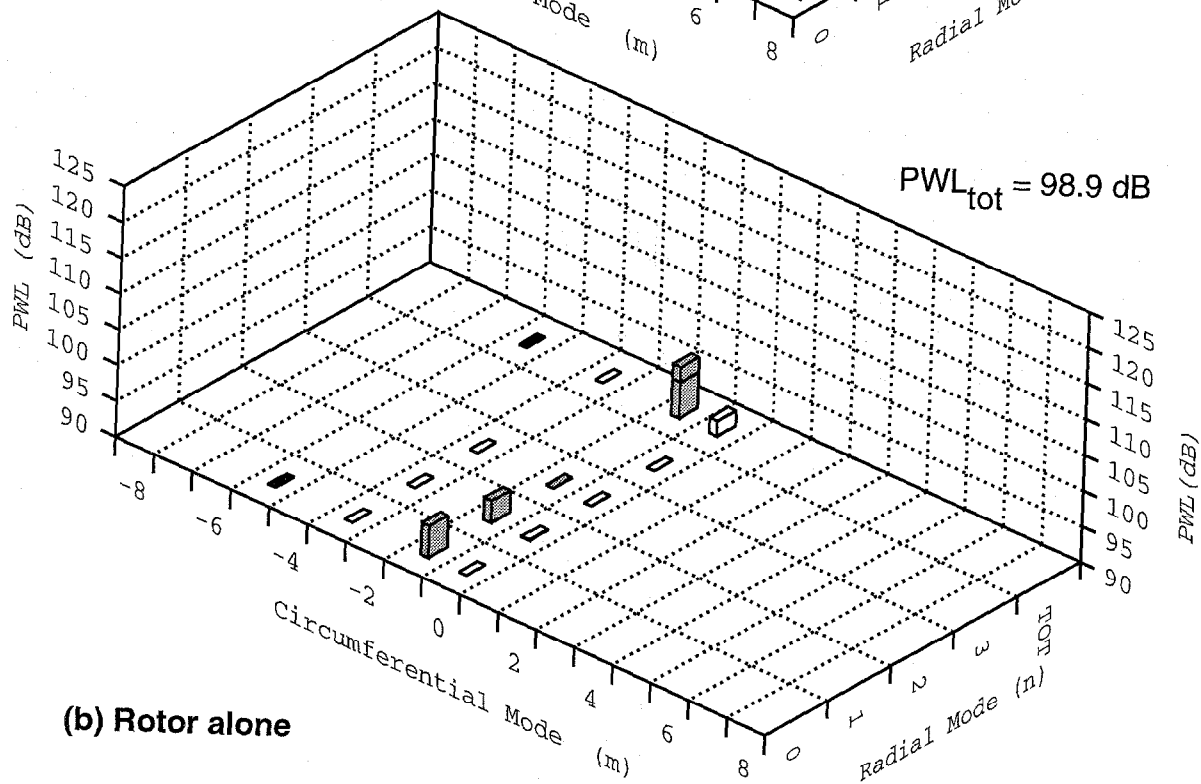
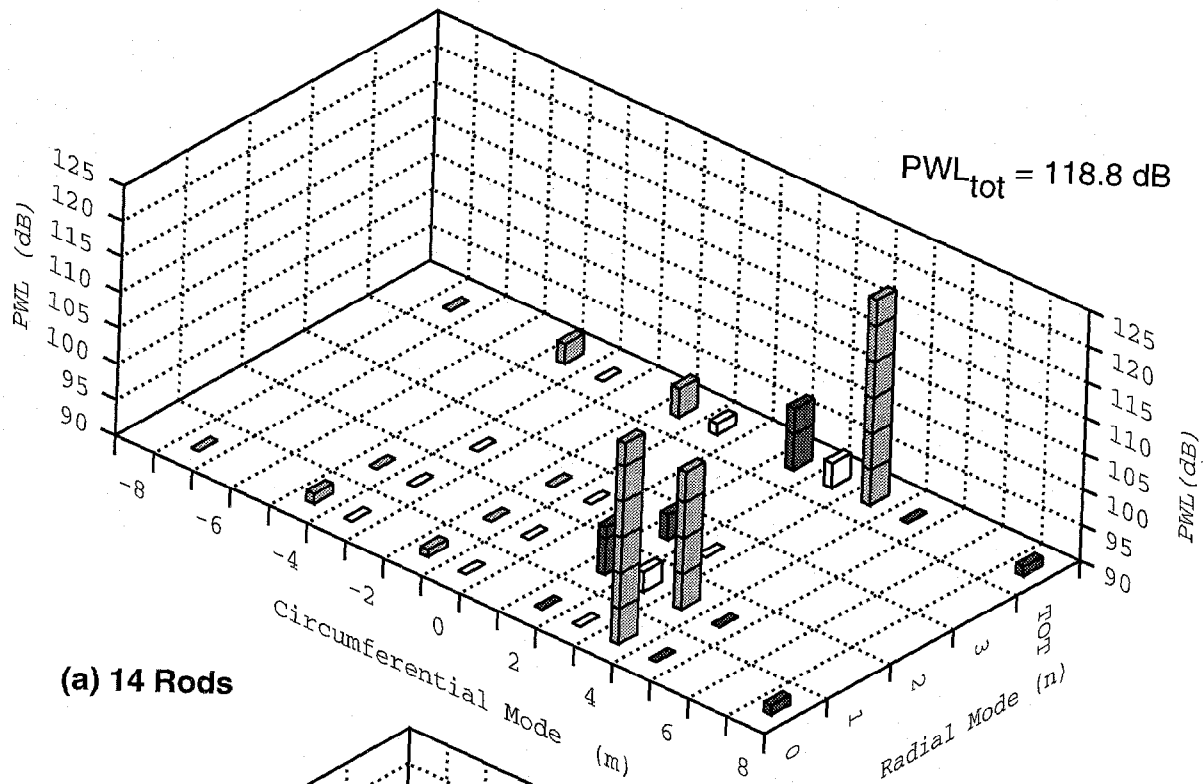


Figure 5. Comparison of Inlet Modal Structure at 2BPF for Rotor Alone and 14 Rod-Rotor Configurations, 1886 RPM.

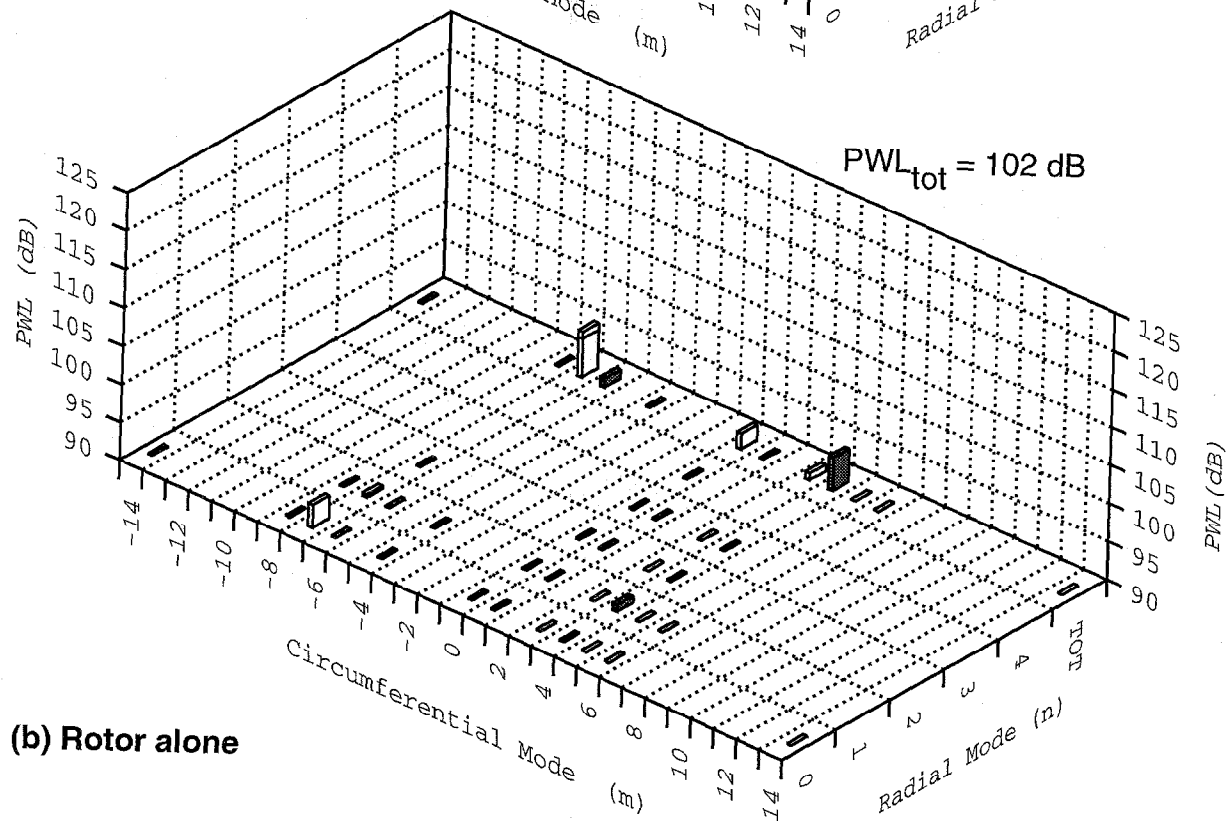
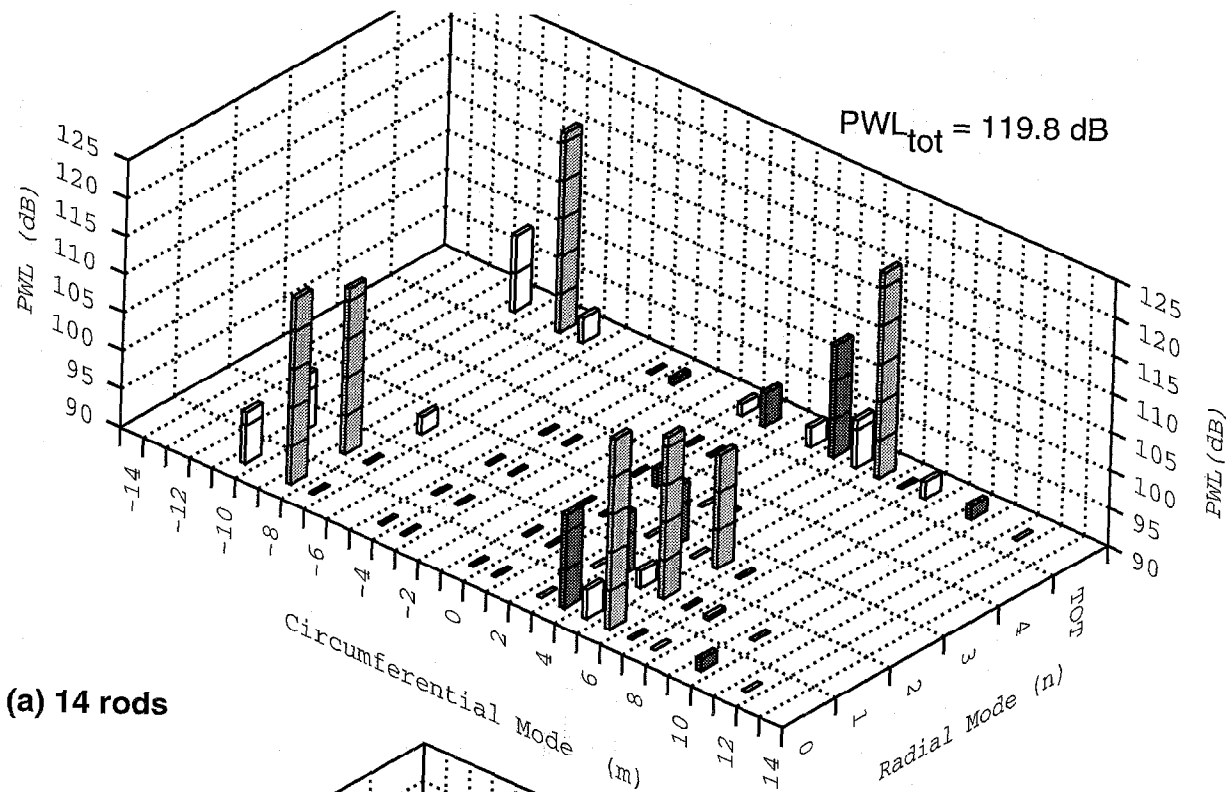


Figure 6. Comparison of Inlet Modal Structure at 3BPF for Rotor Alone and 14 Rod-Rotor Configurations, 1886 RPM.

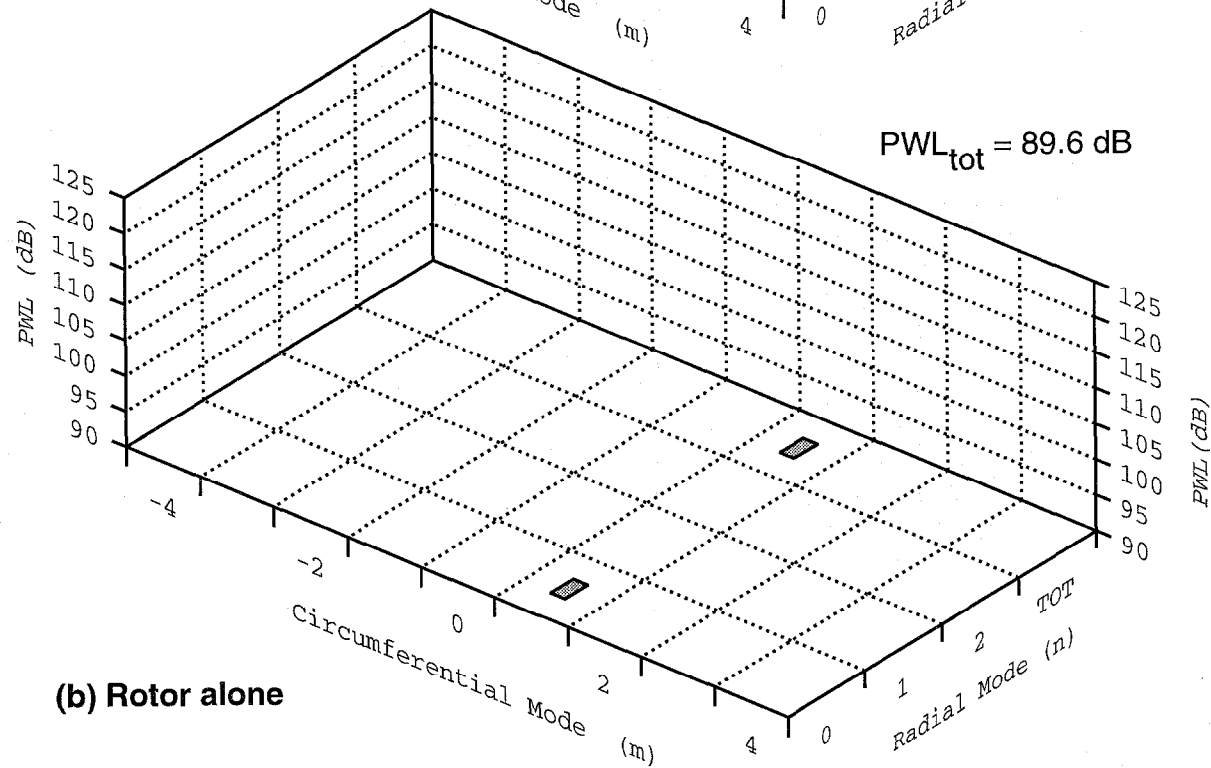
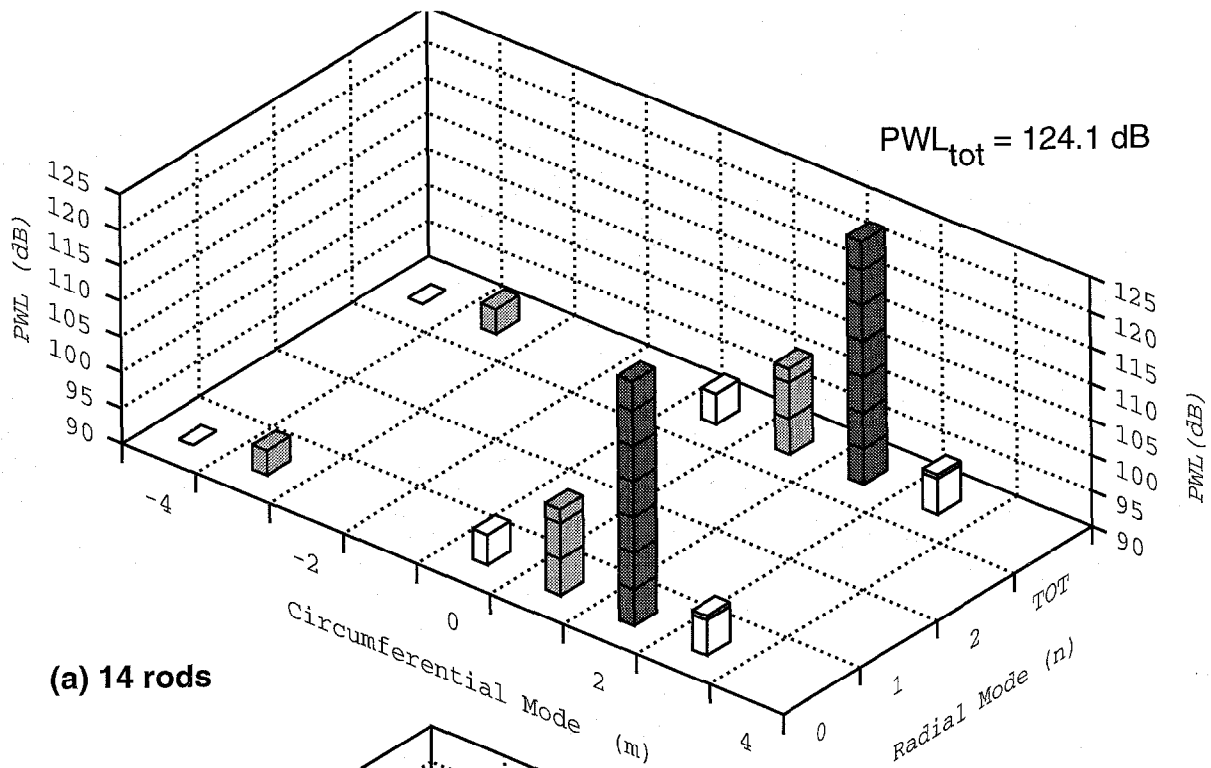


Figure 7. Comparison of Exhaust Modal Structure at BPF for Rotor Alone and 14 Rod-Rotor Configurations, 1886 RPM.

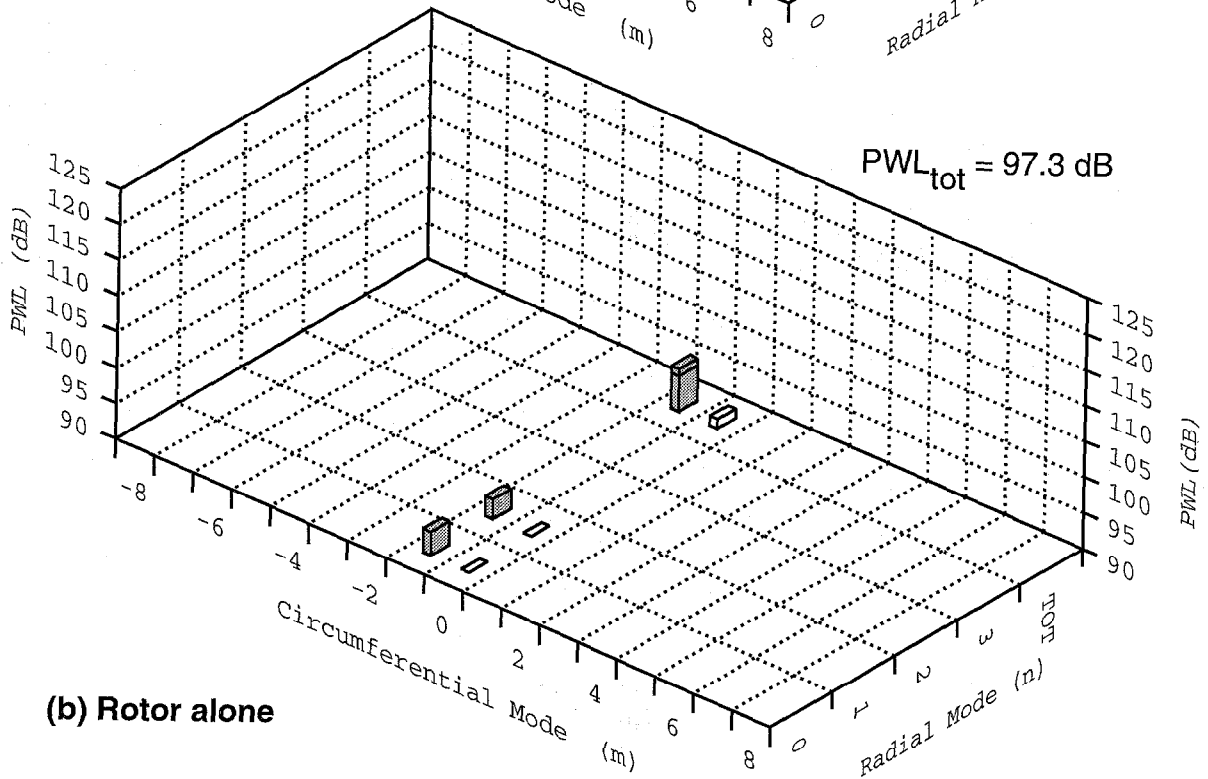
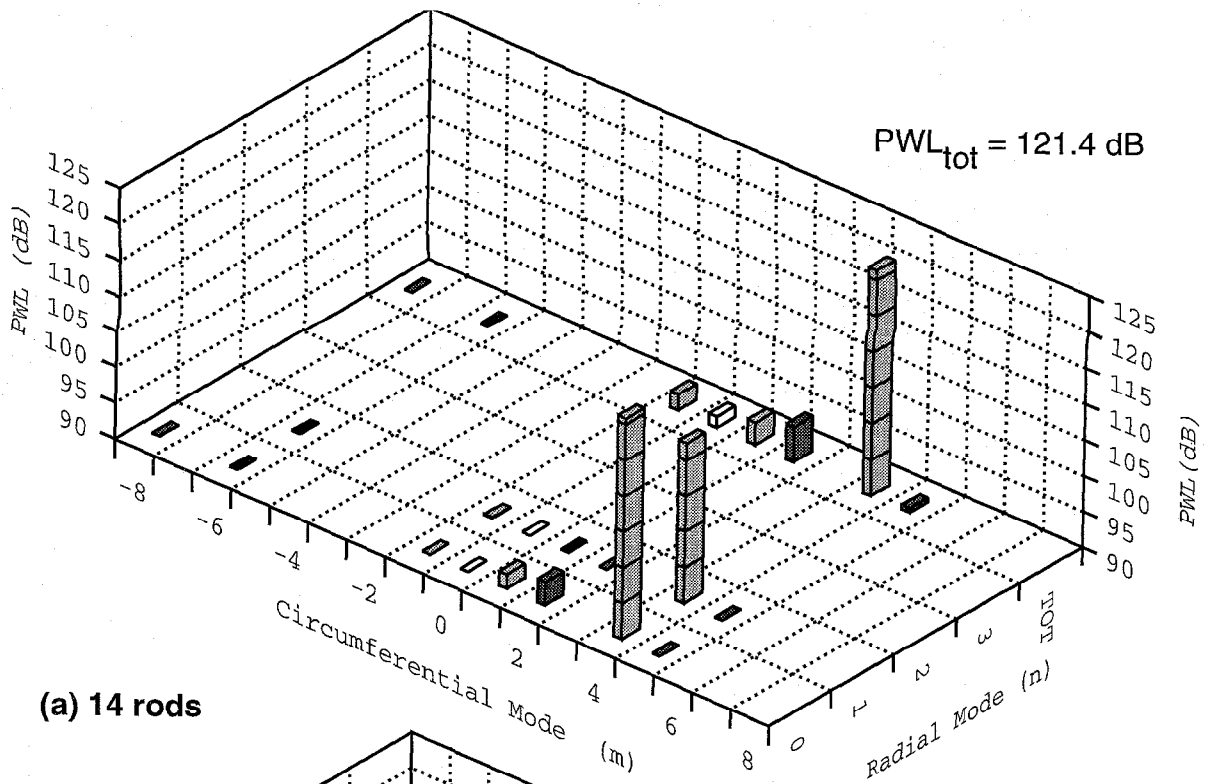


Figure 8. Comparison of Exhaust Modal Structure at 2BPF for Rotor Alone and 14 Rod-Rotor Configurations, 1886 RPM.

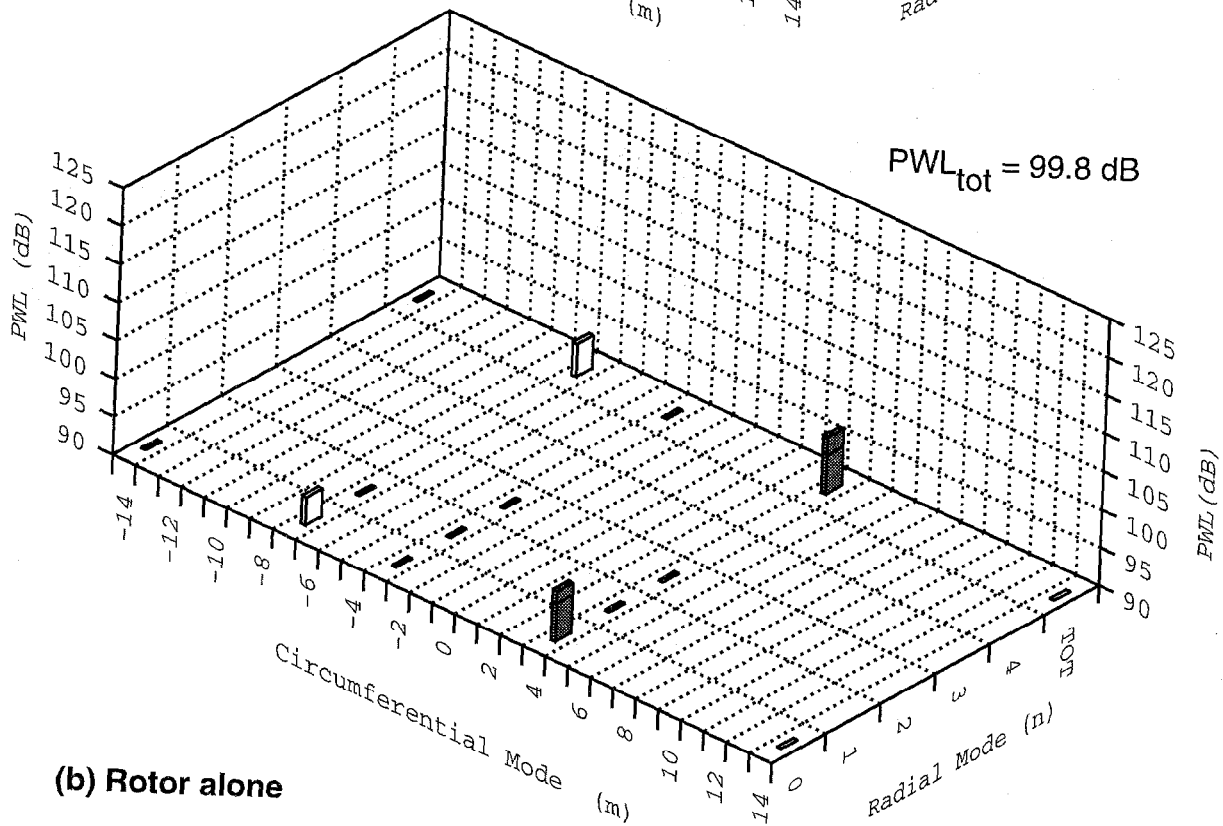
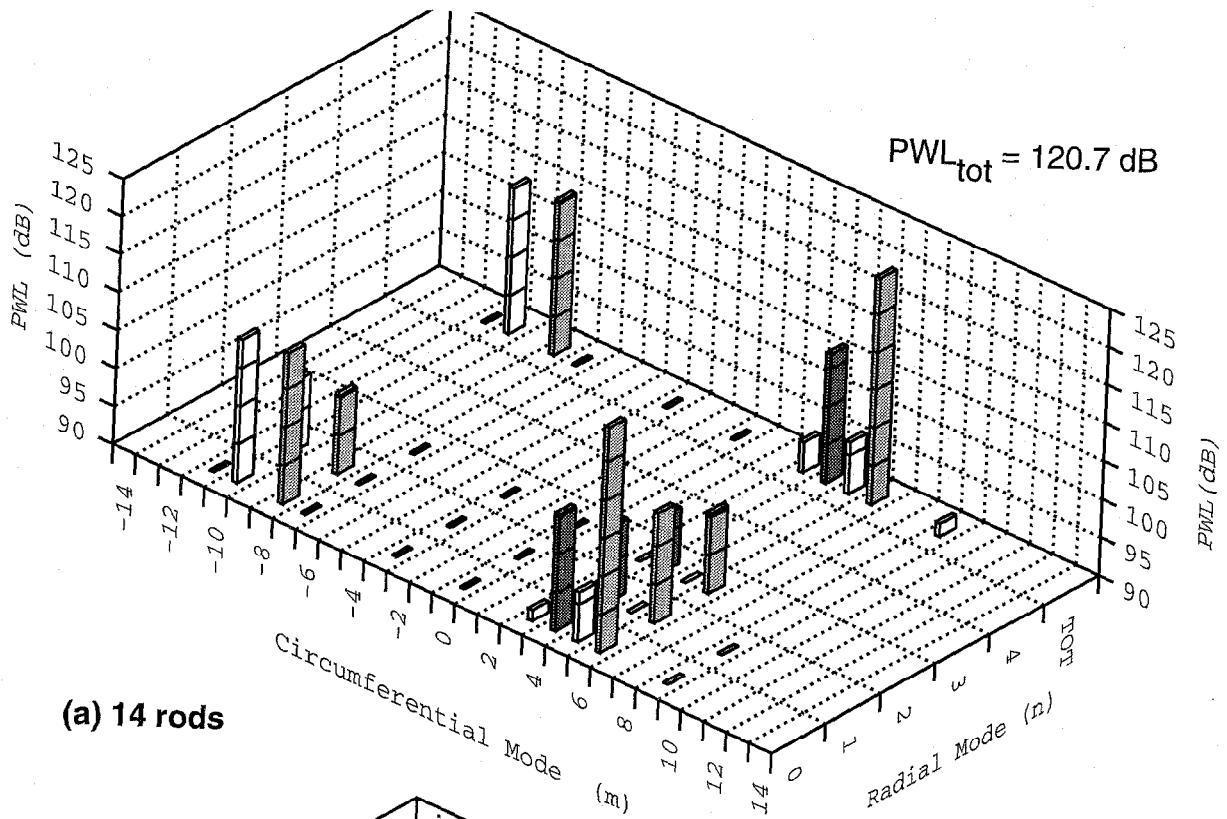
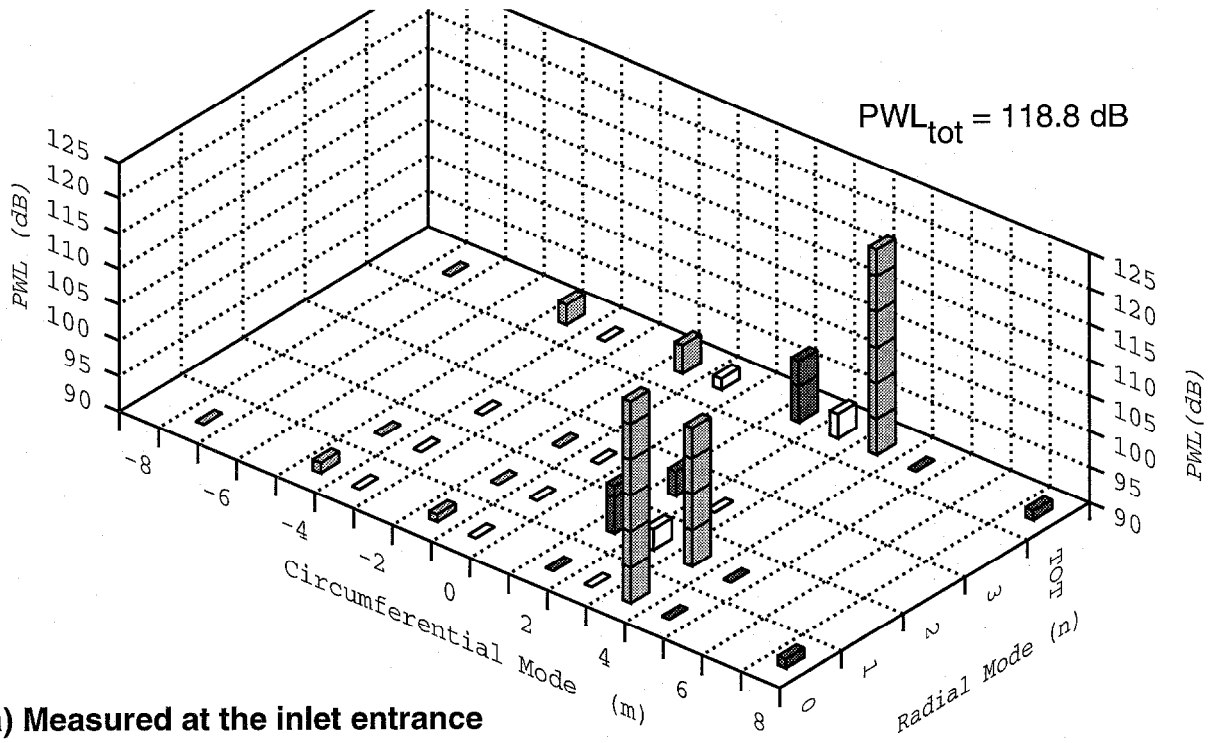
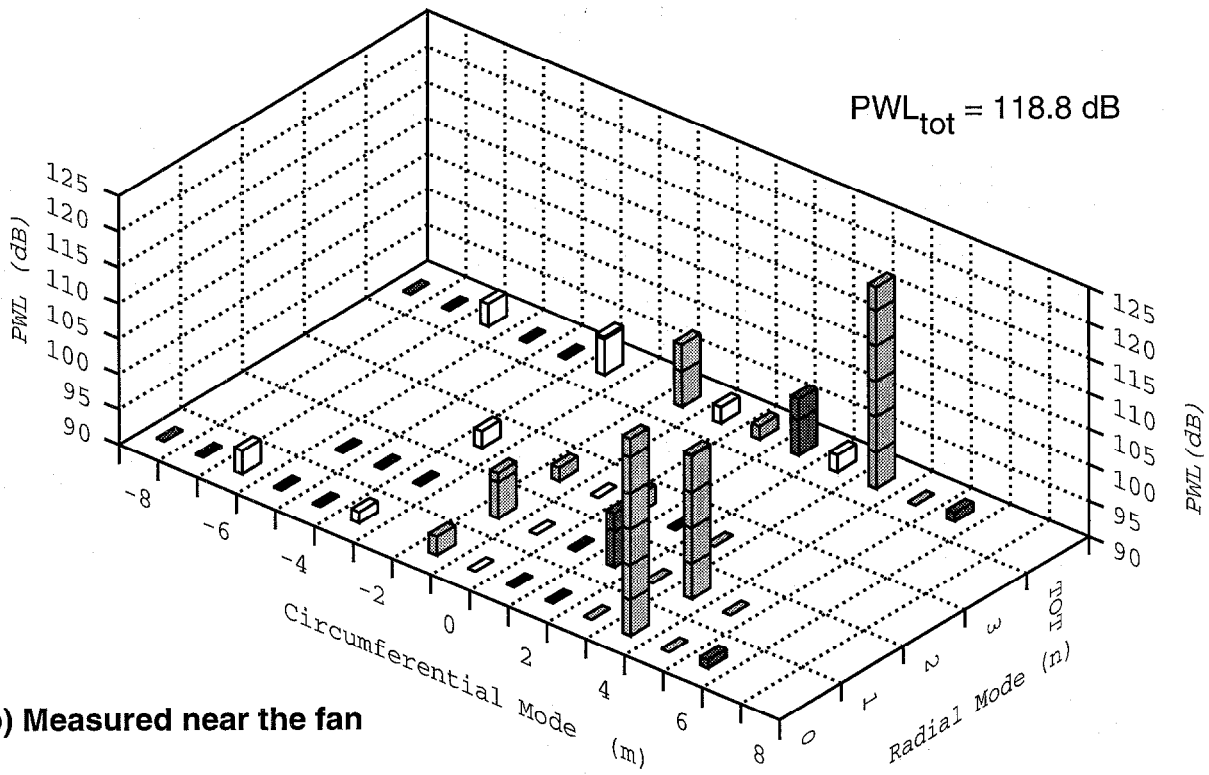


Figure 9. Comparison of Exhaust Modal Structure at 3BPF for Rotor Alone and 14 Rod-Rotor Configurations, 1886 RPM.

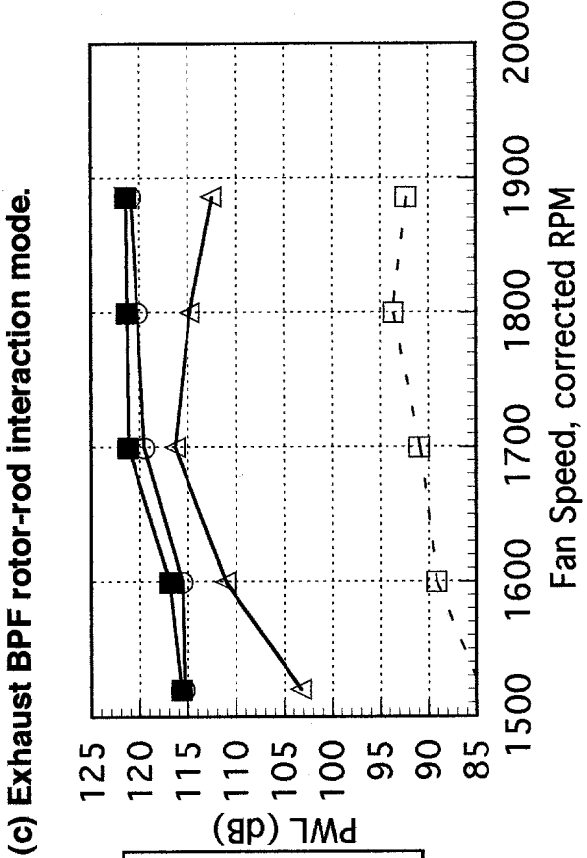
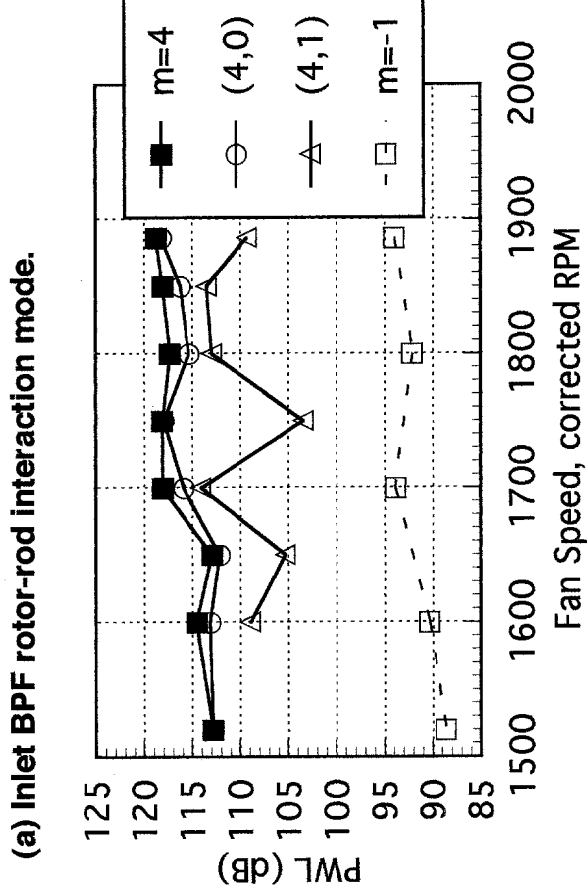
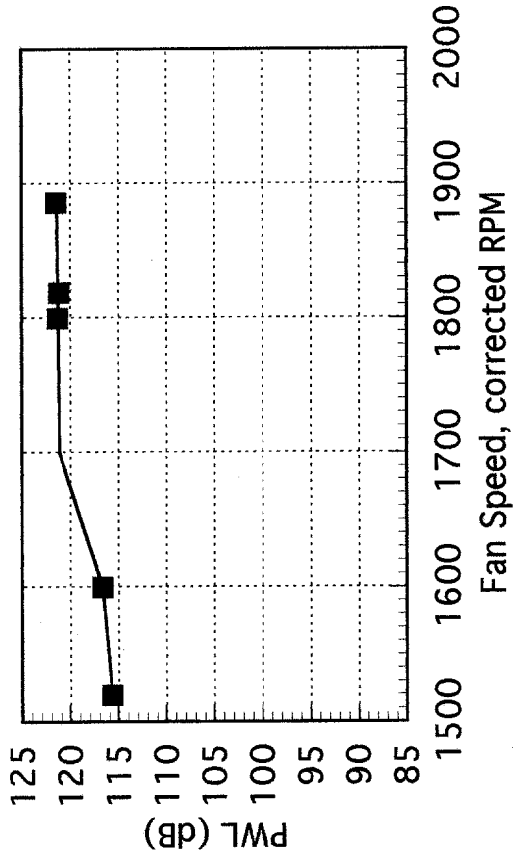
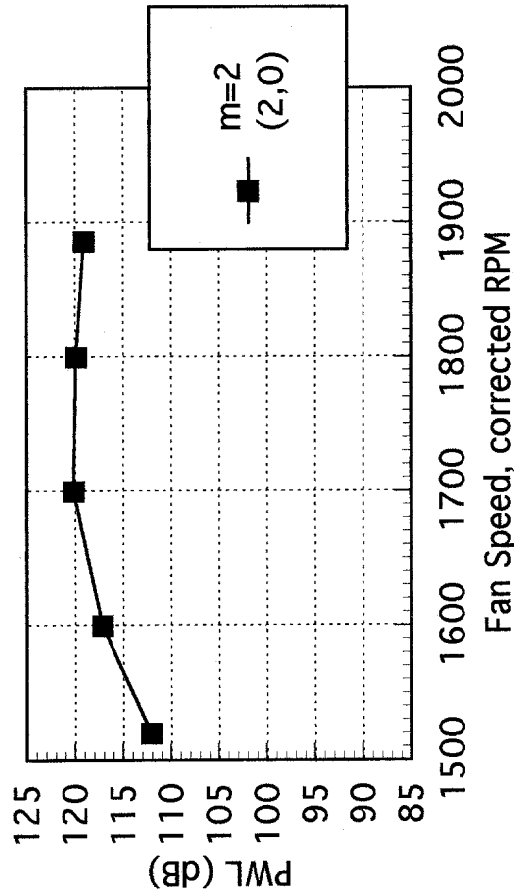


(a) Measured at the inlet entrance



(b) Measured near the fan

Figure 11. Comparison of 2BPF Modal Structure Measured at Two Inlet Locations, 14 rods, 1886 RPM.



(b) Inlet 2BPF rotor-rod interaction modes (m=4) + rotor-ICD modes (m=-1).

(d) Exhaust 2BPF rotor-rod interaction modes (m=4) + rotor-ICD modes (m=-1).

Figure 12. Interaction Mode Power as a Function of Fan Speed, 14 rods.

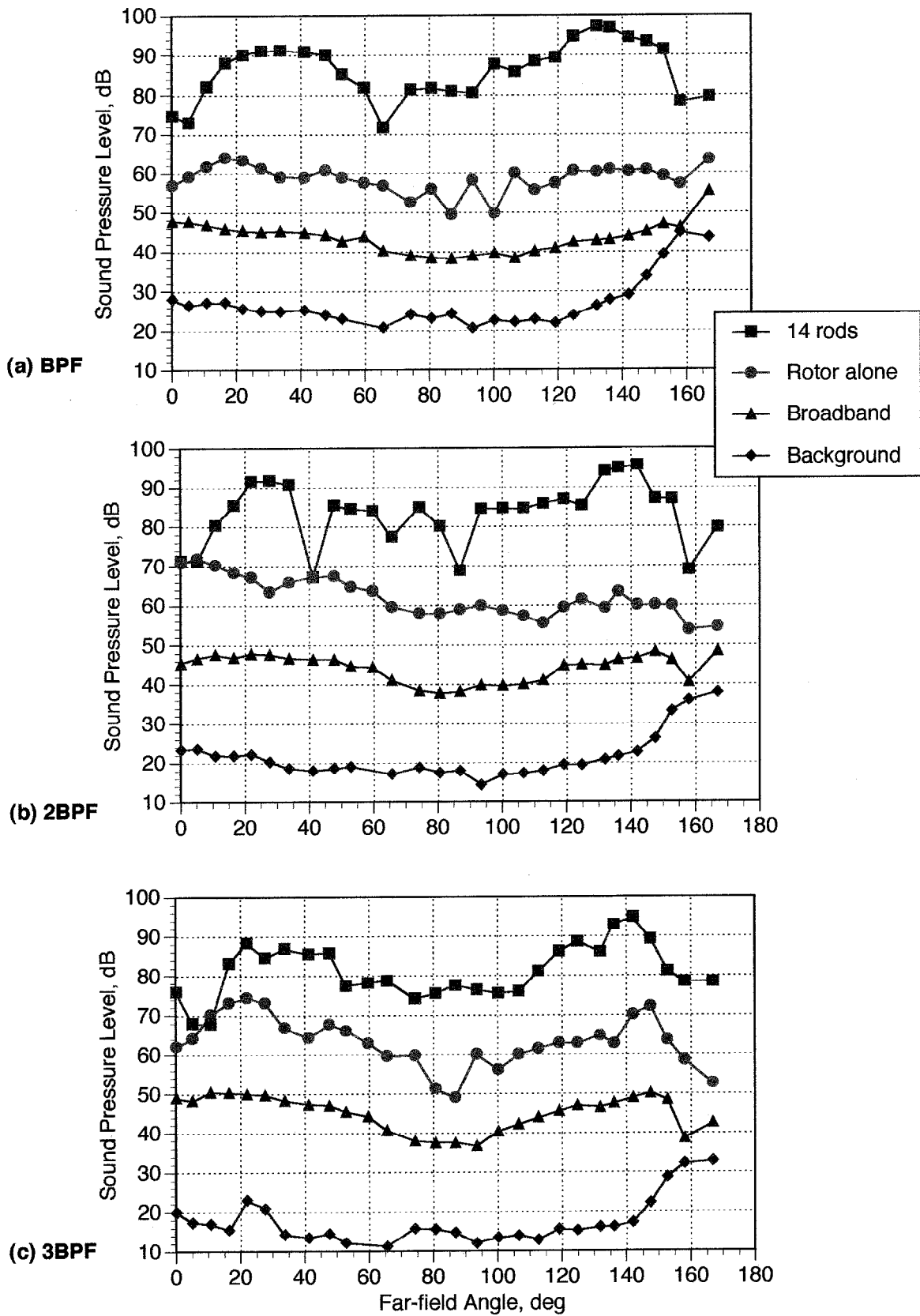


Figure 13. Far-field Directivity Comparison of 14 Rods and Rotor Alone at a Radius of 10 D, 1886 RPM

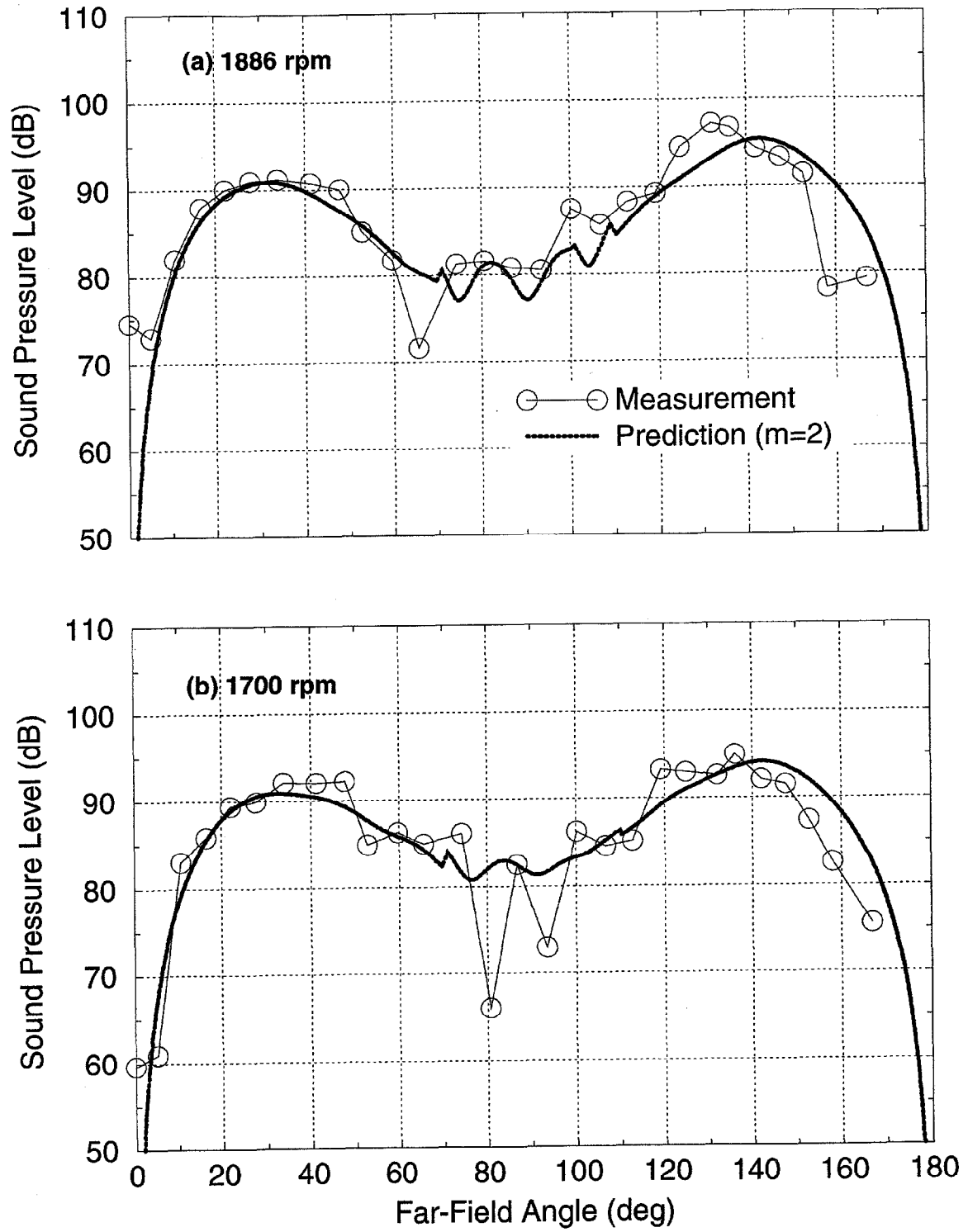


Figure 14 Measured and predicted far-field directivity for 16 blades/14 rods at BPF

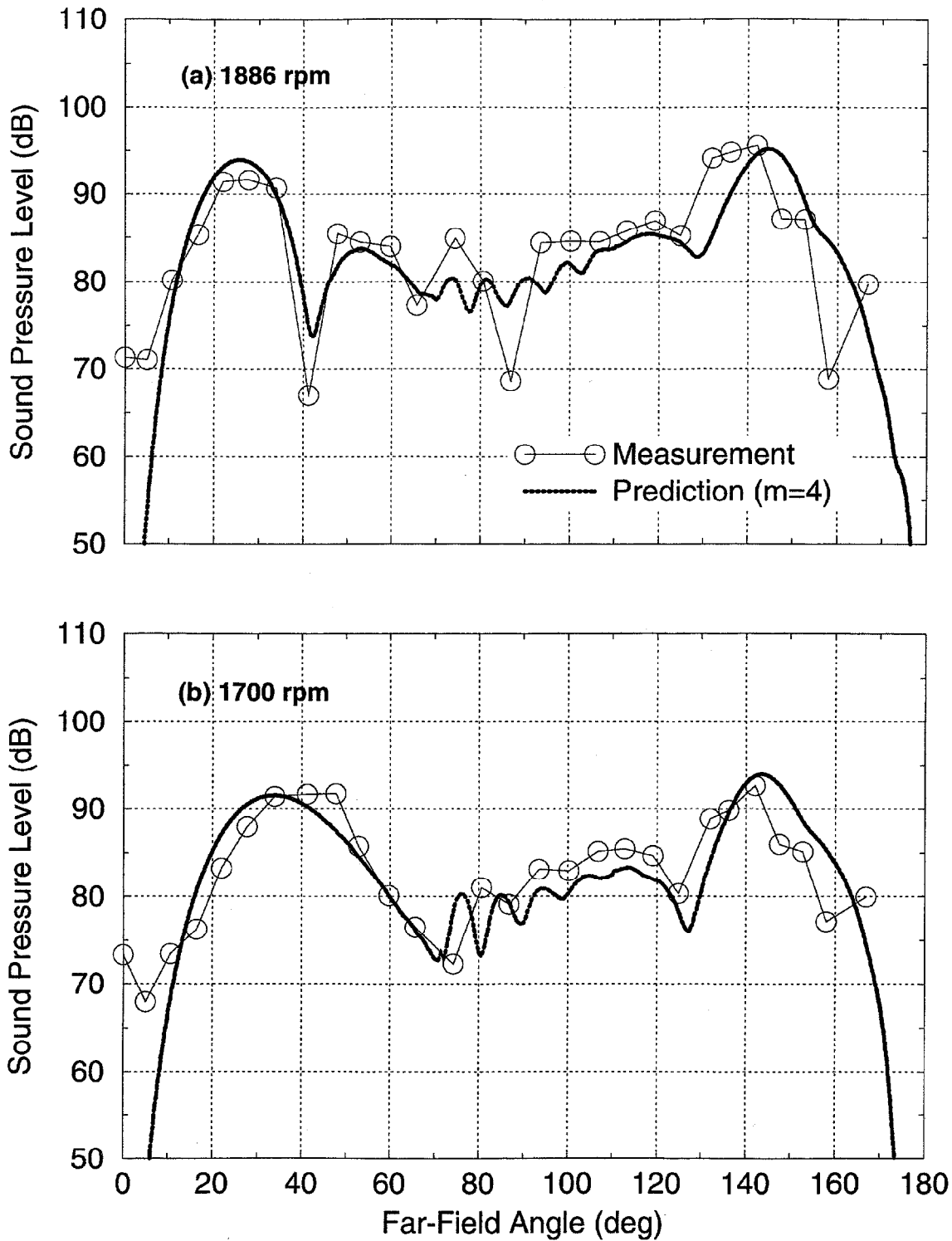


Figure 15 Measured and predicted far-field directivity for 16 blades/14 rods at 2BPF

REPORT DOCUMENTATION PAGE

Form Approved
OMB No. 0704-0188

Public reporting burden for this collection of information is estimated to average 1 hour per response, including the time for reviewing instructions, searching existing data sources, gathering and maintaining the data needed, and completing and reviewing the collection of information. Send comments regarding this burden estimate or any other aspect of this collection of information, including suggestions for reducing this burden, to Washington Headquarters Services, Directorate for Information Operations and Reports, 1215 Jefferson Davis Highway, Suite 1204, Arlington, VA 22202-4302, and to the Office of Management and Budget, Paperwork Reduction Project (0704-0188), Washington, DC 20503.

1. AGENCY USE ONLY (Leave blank)	2. REPORT DATE May 1996	3. REPORT TYPE AND DATES COVERED Technical Memorandum	
4. TITLE AND SUBTITLE A Unique Ducted Fan Test Bed for Active Noise Control and Aeroacoustics Research		5. FUNDING NUMBERS WU-538-03-11	
6. AUTHOR(S) Laurence J. Heidelberg, David G. Hall, James E. Bridges, and M. Nallasamy			
7. PERFORMING ORGANIZATION NAME(S) AND ADDRESS(ES) National Aeronautics and Space Administration Lewis Research Center Cleveland, Ohio 44135-3191		8. PERFORMING ORGANIZATION REPORT NUMBER E-10230	
9. SPONSORING/MONITORING AGENCY NAME(S) AND ADDRESS(ES) National Aeronautics and Space Administration Washington, D.C. 20546-0001		10. SPONSORING/MONITORING AGENCY REPORT NUMBER NASA TM-107213 AIAA-96-1740	
11. SUPPLEMENTARY NOTES Prepared for the Second Aeroacoustics Conference cosponsored by the American Institute of Aeronautics and Astronautics and the Confederation of European Aerospace Societies, State College, Pennsylvania, May 6-8, 1996. Laurence J. Heidelberg, NASA Lewis Research Center; David G. Hall, James E. Bridges, and M. Nallasamy, NYMA, Inc., 2001 Aerospace Parkway, Brook Park, Ohio 44142 (work funded by NASA Contract NAS3-27186). Responsible person, Laurence J. Heidelberg, organization code 2770, (216) 433-3859.			
12a. DISTRIBUTION/AVAILABILITY STATEMENT Unclassified - Unlimited Subject Categories 07 and 71 This publication is available from the NASA Center for AeroSpace Information, (301) 621-0390.		12b. DISTRIBUTION CODE	
13. ABSTRACT (Maximum 200 words) This paper describes a unique, large diameter, low speed, axial fan test bed with an externally supported duct. This fan can be used both to investigate active noise control and for more general fan aeroacoustics research. Several of the features and the design philosophies are presented. The most important feature is the installation of two mode measuring systems that enable the complete modal structure (all circumferential and radial orders) of both the inlet and exhaust ducts to be determined. A sample of data for two configurations, rotor alone and rod/rotor interaction are presented. In-duct modal data for rotor alone reveals minimal extraneous modes that might interfere with any interaction modes being investigated. The rod data shows strong interactions for the expected modes. High resolution spectral and spacial far-field data reveal a directivity pattern consistent with the modal structure. The unique ability to view both far-field and in-duct modal structure makes this test bed will suited for the test and development of fan active noise control systems. The rod modal data was projected to the far-field using a finite element code and compared to the actual far-field data showing an excellent agreement. This not only validates the code but contributes to confidence in the in-duct and far-field data quality.			
14. SUBJECT TERMS Ducted fans; Engine noise; Active control; Acoustic measurement; Aircraft noise; Aeroacoustics; Noise measurement; Noise reduction		15. NUMBER OF PAGES 25	
		16. PRICE CODE A03	
17. SECURITY CLASSIFICATION OF REPORT Unclassified	18. SECURITY CLASSIFICATION OF THIS PAGE Unclassified	19. SECURITY CLASSIFICATION OF ABSTRACT Unclassified	20. LIMITATION OF ABSTRACT